Interleukin-16 inhibits sodium channel function and GluA1 phosphorylation via CD4- and CD9-independent mechanisms to reduce hippocampal neuronal excitability and synaptic activity.

Short title: IL-16 modulates neuronal function.

Shehla U. Hridi, Aimée JPM Franssen, Hui-Rong Jiang and Trevor J. Bushell[1]

(orcid.org/0000-0003-4145-9670)

Strathclyde Institute of Pharmacy and Biomedical Sciences, University of Strathclyde, 161 Cathedral Street, Glasgow G4 0RE, UK.

[1]Corresponding author: Dr Trevor J Bushell, Strathclyde Institute of Pharmacy and Biomedical Sciences, University of Strathclyde, Glasgow G4 0RE, UK. Tel: 0044 141 548 2856, email: trevor.bushell@strath.ac.uk

Abstract

Interleukin 16 (IL-16) is a cytokine that is primarily associated with CD4$^+$ T cell function, but also exists as a multi-domain PDZ protein expressed within cerebellar and hippocampal neurons. We have previously shown that lymphocyte-derived IL-16 is neuroprotective against excitotoxicity, but evidence of how it affects neuronal function is limited. Here, we have investigated whether IL-16 modulates neuronal excitability and synaptic activity in mouse primary hippocampal cultures. Application of recombinant IL-16 impairs both glutamate-induced increases in intracellular Ca^{2+} and sEPSC frequency and amplitude in a CD4- and CD9-independent manner. We examined the mechanisms underlying these effects, with rIL-16 reducing GluA1 S831 phosphorylation and inhibiting Na$^+$ channel function. Taken together, these data suggest that IL-16 reduces neuronal excitability and synaptic activity via multiple mechanisms and adds further evidence that alternative receptors may exist for IL-16.

Abbreviations: AD, Alzheimer's Disease; a[Ca^{2+}]$_i$, astrocytic intracellular calcium; CNS, central nervous system; DIV, days *in vitro*; GluA1, α-amino-3-hydroxy-5-methyl-4-isoxazolepropionic acid receptor subunit A1; HCM, hippocampal conditioned medium; LCF, lymphocyte chemoattractant factor; LCM, lymphocyte conditioned medium; MS, multiple sclerosis; NIL-16; neuronal IL-16; n[Ca^{2+}]$_i$, neuronal intracellular calcium; rIL-16, recombinant mouse IL-16; sEPSC, spontaneous excitatory postsynaptic potential; TNF-α, tumour necrosis factor α.

1. Introduction

Central nervous system (CNS) disorders are growing more prevalent due to the ageing population and are a major global health challenge. Hence, there is a significant drive to improve further our understanding of the aetiologies associated with these disorders in order to develop new therapeutics. Within the last decade, the role of neuroinflammation in CNS disorders has become an area of intense investigation with inflammation shown to play a significant role in many CNS disorders including Alzheimer's disease (AD) and multiple sclerosis (MS) (Laurent et al., 2018; Selles et al., 2018, Zephir, 2018). Whilst the CNS was once considered an immune privileged site, it is now accepted that there is bidirectional communication between the CNS and the immune system, with the innate and adaptive immune system thought to influence CNS development, function and disease progression (Forrester et al., 2018; Stephenson et al., 2018).

Key signalling molecules that are involved in these actions are cytokines, inflammatory mediators that are categorised as either pro- or anti-inflammatory. By binding to their cognate receptors on immune cells, they modulate cell viability, cell proliferation, cytokine secretion, phagocytosis, cell adhesion and cell migration. Apart from coordinating innate and adaptive immune responses throughout the body, cytokines are present in the CNS under physiological and pathophysiological conditions (Louveau et al. 2015, Colonna & Butovsky, 2017). Classically, cytokines only occur within the CNS following release by infiltrating immune cells during inflammatory CNS disorders. However, recent evidence indicates that CNS resident cells including astrocytes, microglia and neurons, produce and release cytokines (Arisi, 2014). These cytokines are involved in a complex crosstalk between several cell types in the CNS and modulate several physiological functions including neurite outgrowth, neurogenesis, synaptic development and synaptic plasticity (Vezzani & Viviani, 2015; de Miranda et al., 2017; Levin & Godukhin, 2018). In addition, elevated levels of inflammatory cytokines, proposed to be involved in disease initiation and progression, are observed in neuroinflammatory diseases including AD, MS and Parkinson's disease (Martins et al., 2011, Garcia-Esparcia et al., 2014, Zheng et al., 2016). Much of our knowledge regarding cytokines and brain function is related to the pro-inflammatory cytokines, interleukin-1β (IL-1β), IL-6 and tumour necrosis factor-α (TNF-α). Indeed, these cytokines are linked

to the modulation of synaptic plasticity, learning and memory as well as disease development (Donzis & Tronson, 2014; Gruol, 2015; Vezzani & Viviani, 2015)

In addition to these well-studied cytokines, other cytokines are linked to inflammation-related CNS disorders, but their exact functional role remains unclear. One such cytokine is IL-16, originally known as lymphocyte chemoattractant factor (LCF). IL-16 was identified as a T-cell-derived cytokine that induces CD4-dependent migration and proliferation of immune cells (Center and Cruickshank., 1982, Parada et al., 1998, Liu et al., 1999), but we now know that IL-16 is also produced by other immune cells including B cells and monocytes (Kaser et al., 2000; Elssner et al., 2004). In addition, we recently revealed that immune cell-derived IL-16 is neuroprotective against kainate- and oxygen-glucose deprivation (OGD)-induced excitotoxicity in organotypic slice cultures (Shrestha et al., 2014). Finally, in keeping with the intense interest in the role of cytokines in CNS disorders, recent studies have proposed that IL-16 plays a role in AD, relapsing MS and experimental autoimmune encephalomyelitis (EAE, Anvar et al., 2015; Skundric et al., 2015). Interestingly, in addition to its role in inflammation, a neuronal variant exists as a longer splice variant of the immune cell-derived IL-16 precursor protein, pro-IL-16, with two extra PDZ domains in the N-terminal region (Kurschner & Yuzaki., 1999). Neuronal IL-16 (NIL-16), which is selectively expressed in hippocampal and cerebellar neurons, is cleaved by caspase-3 similar to pro-IL-16 in immune cells and results in the release of mature IL-16 (Kurschner & Yuzaki., 1999). Furthermore, NIL-16 induces the upregulation of the transcription factor *c-fos*, (Kurschner and Yuzaki, 1999; Fenster et al., 2010), enhances neurite outgrowth (Fenster et al., 2010) and interacts with neurotransmitter receptors and several ion channel proteins (Kurschner & Yuzaki., 1999; Fenster et al., 2007).

Despite these recent findings, whether IL-16 modulates hippocampal neuronal excitability and synaptic transmission remains unclear. In the present study, we reveal that in mouse hippocampal cultures, recombinant mouse IL-16 (rIL-16) impairs glutamate-induced increases in neuronal intracellular calcium ($n[Ca^{2+}]_i$) and inhibits the frequency and amplitude of spontaneous excitatory postsynaptic currents (EPSCs). These IL-16 mediated effects, which in contrast to previous reports are CD4-

4

independent, are associated with a reduction in Na$^+$ channel function and reduced GluA1 phosphorylation.

2. Materials and Methods

All experimental procedures were performed in accordance with UK legislation including the Animals (Scientific Procedures) Act 1986 and with approval of the University of Strathclyde Animal Welfare and Ethical Review Body (AWERB).

2.1 Mouse primary hippocampal culture: Mouse primary hippocampal cultures were prepared as described previously (Abdul Rahman et al., 2016). Briefly, C57BL/6J pups (1-2 days old) were sacrificed by cervical dislocation and decapitated. Under sterile conditions, the hippocampi were removed, triturated and the resulting dissociated cells were plated at a density of 5.5×10^5 cells mL^{-1} onto 13 mm coverslips or 6 well plates both coated with poly-L-lysine (0.01 mg mL^{-1}; Sigma, UK). Cultures were incubated in culture medium consisting of Neurobasal-A medium (phenol red free for Ca^{2+} imaging, Invitrogen, Paisley, UK) supplemented with 2% (v/v) B-27 serum-free supplement (Invitrogen, Paisley, UK) and 2 mM L-glutamine (Invitrogen, Paisley, UK) and maintained in a humidified incubator at 37ºC/5% CO2 for 11-14 days *in vitro* (DIV) prior to functional studies. Cytosine β-D-arabinofuranoside (1µM; Sigma, UK) was added at 5 DIV to prevent further glial cell proliferation. All experiments were performed on cells taken from at least three separate cultures obtained from different animals.

2.2 Lymphocyte preparation and ELISA: Popliteal, inguinal, axillary, brachial, cervical and mesenteric lymph nodes were harvested from C57BL/6J mice (8-10 weeks old) and transferred to Neurobasal-A culture medium. The lymph nodes were homogenised, passed through a cell strainer (70µm; Corning Falcon, UK) and transferred to a 15 mL sterile tube, then centrifuged at 400 x g for 5 min. Cells were washed twice and plated at a density of 4×10^6 cells mL^{-1} and maintained in hippocampal conditioned medium (HCM; culture medium from 11-14 day old hippocampal cultures) in a humidified incubator at 37°C/5% CO_2 for 18 hours. Lymphocyte conditioned medium (LCM) was then collected, with mouse IFN-γ and IL-16 protein levels determined by ELISA according to manufacturer's

instructions (eBiosciences and R&D Systems UK, respectively) using the following capture antibodies (anti-mouse IFN-γ; #14-7313-85 and rat anti-mouse IL-16; #842373) and detection antibodies (biotinylated anti-mouse IFN-γ, #13-7312-85 and biotinylated goat anti-mouse IL-16, #842374).

2.3 Ca^{2+} imaging: Calcium imaging experiments were performed on hippocampal cultures (11-14 DIV) as previously described (Tinning et al., 2018). Prior to imaging, cells were loaded with Fura-2 AM (1 μM; Invitrogen, UK) for 1 hour in a humidified incubator at 37°C/5% CO_2, while simultaneously being treated with either vehicle or rIL-16 (300 pg mL^{-1}, #RP8610; Thermo Fisher, UK). Cultures were then washed three times in HEPES-buffered saline (HBS) consisting of the following (in mM): NaCl 140, KCl 5, $MgCl_2$ 2, $CaCl_2$ 2, HEPES 10, D-glucose 10, pH 7.4 ± 0.02, 310 ± 2 mOsm. Throughout imaging, cultures were perfused with HBS at a rate of 3–3.5 mL min^{-1} with all drug solutions being added via the perfusate. Cultures were placed in a perfusion bath under a 20×/0.5 water dipping objective lens (Olympus UMPlanFl, Tokyo, Japan) on an upright widefield epifluorescence microscope (Olympus BXW51, Japan) with ratiometric images (350/380 nm; OptoLED, Cairn Research, UK) taken at 0.5 Hz from the neuronal soma and astrocytes using WinFluor imaging software (J. Dempster, University of Strathclyde). Cells were identified as neurons and astrocytes based on their morphological characteristics and their response to ADP and/or high extracellular KCl.

2.5 Electrophysiology: Mouse primary hippocampal cultures (11-14 DIV) were treated with vehicle, rIL-16 (300 pg mL^{-1}, #RP8610; Thermo Fisher, UK) or denatured rIL-16 (rIL-16 boiled for 1 hour at 90°C) for 1 hour in a humidified incubator at 37°C/5% CO_2. Cultures were then washed with HBS and placed in a recording chamber and perfused continuously with HBS (1–2 mL min^{-1}). Fire polished borosilicate glass microelectrodes (4-6 MΩ, Harvard Apparatus, UK) were filled with an internal solution containing (in mM): $KMeSO_3$ 130, KCl 20, HEPES 10, EGTA 0.5, Mg-ATP 4 and Na-GTP 0.3, pH 7.2 ± 0.02, 290 ± 2 mOsm. All experiments were performed at room temperature (21-23°C) using an Axopatch-200B amplifier (Molecular Devices, USA) connected to a personal computer interfaced with Digidata 1322A interface (Molecular Devices, USA) and captured using Clampex 9.2

software (Molecular Devices, USA). For current–voltage relationships, cells were held at -70mV in voltage clamp mode with 10 mV increments for 200 ms at 10 s intervals with Na^+ current measured as the peak inward current at each voltage step and the K^+ current measured as the peak steady state outward current at the last 10 ms of each voltage step. Spontaneous excitatory postsynaptic currents (sEPSCs), digitized at 5 kHz, were recorded at -70 mV for 3-minute periods in voltage-clamp mode. Data were analysed offline using Clampfit 10.2 software (Molecular Devices, USA) and MiniAnalysis software (Synaptosoft, USA).

2.6 Immunostaining

2.6.1 Immunohistochemistry: C57BL/6J mice (6-8 weeks old) were sacrificed by cervical dislocation, perfused with phosphate buffered saline (PBS) following which the brain was removed and snap frozen in OCT. Brain sections (7μm) were cut using a cryostat (Shandon, Thermo Fisher, UK) and then stained with a primary antibody against IL-16 (1:400, #PA5-20670; Thermo Fisher, UK) or CD4 (RM4-5, 1:400, 14-0042-85; eBioscience, UK), followed by incubation with an appropriate biotin-conjugated secondary antibody (#550338; BD Pharmingen, UK), horseradish peroxidase and ImmPACT^{TM} AMEC red peroxidase substrate (Vector Laboratories, UK). Isotypes with matching IgG were used as negative controls for all antibody staining. Slides were visualized using a Nikon Eclipse 50 microscope with a Nikon Digital Sight DS-U3 camera using NIS Element F3.2 imaging software (Nikon Instruments, UK).

2.6.2 Immunocytochemistry: Mouse primary hippocampal cultures (11-14 DIV) were fixed with ice-cold 4% (v/v) paraformaldehyde for 10 minutes, followed by ice-cold 100% methanol for 10 minutes. Subsequently, cells were permeabilised with Triton-X (0.01% (v/v), Sigma, UK) in blocking solution (5% foetal bovine serum (FBS) v/v and BSA (0.01 g mL^{-1}) in PBS, all Sigma, UK) for 10 minutes, followed by incubation in blocking solution alone for a further 20 minutes. Cultures were then incubated with primary antibodies against MAP2 (1:500, #AB5543; Millipore, UK), GFAP (GA5, 1:500, #3670; Cell Signaling Technologies, The Netherlands), CD4 (RM4-5, 1:400, 14-0042-85; eBioscience, UK) and CD45 (1:5000, # Ab10558; Abcam, UK) diluted in blocking solution at 4°C overnight. The cells

were then washed with blocking solution and incubated with the corresponding fluorescently-conjugated secondary antibodies (Alexa Fluor 488 and Alexa Fluor 555, 1:200, Thermo Fisher, UK) in blocking solution for 1 hour at room temperature. Cultures were then washed and images acquired using an Olympus BXW51 microscope with a Q-imaging digital camera and WinFluor v3.4.4 imaging software (J. Dempster, University of Strathclyde).

2.7 Western blot: Mouse primary hippocampal cultures (11-14 DIV) grown in 6 well plates were treated with either vehicle or rIL-16 (300 pg mL^{-1}, #RP8610, Thermo Fisher, UK) for 1 hour in a humidified incubator at 37°C/5% CO_2, then washed in ice-cold PBS and lysed in lysis buffer consisting of (in mM): Tris 50, NaCl 150, EDTA 1, Triton X-100 (1% v/v), deoxycholate (0.05% v/v), pH 7.4 ± 0.02, containing a phosphatase and protease inhibitor cocktail (Sigma Aldrich). Lysates were then centrifuged at 16,000 rpm for 10 minutes. Equal amounts of protein were heated to 95ºC in SDS sample buffer for 5 minutes, resolved by SDS-PAGE and transferred to nitrocellulose for immunoblotting analysis. Blots were incubated overnight at 4°C with primary antibodies against total GluA1 (1:1000, #ab109450; Abcam, UK), GluA1 phospho S845 (1:1000, #ab76321; Abcam, UK), GluA1 phospho Ser831 (1:1000, #04-823; Millipore, UK), pan sodium channel (1:500, #SAB4502713; Sigma, UK), CD4 (RM4-5, 1:400, 14-0042-85; eBioscience, UK) or CD9 (1:500, #ab92726; Abcam, UK). Membranes were then washed in PBS-Tween (0.1%) for 20 minutes, followed by incubation with corresponding secondary antibodies (IR dye, 1 hour, 1:10,000; LI-COR, UK). Blots were scanned using an Odyssey scanner (LI-COR, UK) and bands were analysed and quantified using Image Studio Live 5.2 software (LI-COR, UK).

2.8 Statistics: All data are expressed as mean ± S.E.M. Data were compared by unpaired Student's t-tests, one-way or two-way analysis of variance with Bonferroni's comparison as appropriate, with differences considered significant when $P < 0.05$.

3. Results

3.1 IL-16 reduces pharmacologically-induced increases in neuronal but not astrocytic intracellular Ca^{2+}.

In agreement with our previous findings (Shrestha et al., 2014), conditioned media from mouse lymphocyte preparations contains IL-16. Following an 18h incubation, LCM contains 360 ± 51 pg mL^{-1} (p<0.001 vs HCM, n=3 hippocampal cultures; Fig 1A) whereas in contrast, IL-16 is undetectable in HCM. Furthermore, we confirmed that other cytokines, including IFN-γ, were below detectable levels under our experimental conditions. Hence, we utilised rIL-16 (300 pg mL^{-1}) to determine the consequence of IL-16 exposure on astrocytic and neuronal function. Acute application of rIL-16 (300 pg mL^{-1}, 5 min) did not alter n[Ca^{2+}]$_i$ levels (n=125) when compared to acute vehicle application (n=125, Fig. 1B & C). In contrast, glutamate-induced increases in n[Ca^{2+}]$_i$ ($78.9 \pm 7.0\%$ of vehicle control, n=101 neurons, p<0.05) were significantly impaired following rIL-16 (300 pg mL^{-1}, 1h, Fig. 1D) exposure. However, KCl-induced increases in n[Ca^{2+}]$_i$ were unaffected ($115.1 \pm 6.3\%$ of vehicle control, n=101 neurons, Fig. 1D) as were glutamate- and ADP-induced increases in a[Ca^{2+}]$_i$ (glutamate: $92.4 \pm 14.4\%$ of vehicle control, ADP: $89.5 \pm 10.8\%$ of vehicle control, n=25, Fig. 1E) following rIL-16 treatment.

3.2 rIL-16 treatment significantly reduces sEPSC frequency and amplitude and decreases GluA1 S831 phosphorylation.

Having established that rIL-16 impairs glutamate-induced n[Ca^{2+}]$_i$ elevations, we investigated the effect of rIL-16 exposure on synaptic activity by monitoring sEPSCs. rIL-16 (300 pg mL^{-1}, 1h) impaired sEPSC frequency to $21.6 \pm 6.4\%$ of vehicle control (n=8, p< 0.001. Fig. 2A-C), an effect that was absent when rIL-16 was denatured (dIL-16) prior to application ($97.0 \pm 16.0\%$ of vehicle control, n=6 neurons, Fig. 2A-C). In addition, rIL-16 exposure reduced sEPSC amplitude ($58.3 \pm 6.0\%$ of vehicle control, n=8 neurons, p<0.05, Fig. 2A, B & D) with dIL-16 exposure having no effect ($99.5 \pm 7.2\%$ of vehicle control, n=6 neurons). With IL-16 significantly reducing both the frequency and amplitude of sEPSCs compared to vehicle controls, we examined GluA1 subunit expression and its phosphorylation state

following exposure to rIL-16. GluA1 S831 phosphorylation was decreased in rIL-16 (300pg mL^{-1}, 1h) treated cultures (54.8 ± 6.7% of vehicle control, n=3, p<0.05, Fig. 2E & F) whereas total GluA1 (105.1 ± 27.4% of vehicle control, n=3) and GluA1 S831 phosphorylation (74.1 ± 19.3% of vehicle control, n=3) were unaffected by rIL-16 treatment.

3.3 rIL-16 reduces Na$^+$ channel function but not expression in mouse hippocampal neurons.

Having established that rIL-16 impairs sEPSC frequency and amplitude, we examined whether IL-16 modulation of Na$^+$ and K$^+$ channel function also contributed to these effects. rIL-16 (300 pg mL^{-1}, 1h, n=16) significantly impaired Na$^+$ current density (F=37.74, P<0.001, Fig. 3A & C) compared to vehicle controls (n=15) with peak Na$^+$ current density (at -40mV) being 9.7 ± 1.8% of vehicle control (n=16, p<0.001, Fig. 3A & C). rIL-16-induced inhibition of Na$^+$ current density was partially reversed upon a 3h washout (n=9, F=4.63, P<0.05) with peak Na$^+$ current density being 40.5 ± 6.9% of vehicle control (n=16, P<0.05, Fig. 3C). Analogous to the effects observed on sEPSC frequency and amplitude, exposure to dIL-16 had no effect on Na$^+$ current density with peak Na$^+$ current density being 103.2 ± 11.1% of vehicle control (n=9, Fig. 3C). In contrast to the effects of IL-16 on Na$^+$ current density, K$^+$ current density was unaffected following rIL-16 exposure with peak K$^+$ current density (at +30mV) being 82.6 ± 16.4% of vehicle control (Fig. 3B & D). Having established that rIL-16 significantly reduced Na$^+$ current density, we examined whether this effect is due to altered Na$^+$ channel expression. However, rIL-16 treatment (300pg mL^{-1}, 1h) revealed no change in total Na$^+$ channel expression (89.8 ± 8.2% of vehicle control, n=3, Fig. 2E & F) when compared to vehicle control.

3.4 IL-16 actions in primary hippocampal cultures is CD4- and CD9-independent.

Having shown that IL-16 exposure impairs neuronal excitability and synaptic activity and given that IL-16 is proposed to mediate its effects via CD4-dependent and -independent mechanisms as well as potentially via CD9 (Kurschner and Yuzaki, 1999; Fenster et al., 2010; Yadav et al., 2010; Blake et al., 2018), we examined CD4 and CD9 expression in our primary hippocampal cultures. Using immunocytochemistry, we observed CD4 expression in neither astrocytes nor neurons under our experimental conditions (Fig. 4A-D), whereas positive CD4 staining was evident in control lymphocyte

preparations (Fig. 4E-G). Furthermore, both CD4 and CD9 protein expression was completely absent from our hippocampal cultures when examined using western blots (Fig. S1). In addition, we also examined IL-16 expression in the brain. In agreement with previous findings regarding NIL-16 (Kurschner and Yuzaki, 1999), we observed IL-16 expression in the hippocampus and cerebellum, but in many other brain regions as well. IL-16 expression was present in all hippocampal sub-regions including the dentate gyrus (DG) and CA1-CA4 regions (Fig. 4H & I). In contrast, CD4 staining was absent from all hippocampal regions and from all brain regions examined (Fig. 4J & K).

4. Discussion

In the present study, we show that IL-16 impairs glutamate-induced increases in neuronal intracellular calcium and reduces synaptic activity in mouse hippocampal neurons, effects that are independent of its proposed receptors, CD4 and CD9. Furthermore, we provide evidence that reduced GluA1 phosphorylation and an inhibition of Na^+ channel function are potential mechanisms that may underlie these IL-16-mediated effects.

4.1. IL-16 impairs glutamate-induced increases in neuronal intracellular Ca^{2+} levels.

In agreement with our previous studies, IL-16 levels were elevated in LCM compared to hippocampal media controls, with other cytokine levels being below detectable levels (Shresha et al., 2014; Ritchie et al., 2018). Hence, we utilised rIL-16 at these quantified levels to examine the consequence of IL-16 exposure on neuronal excitability and synaptic activity in order to give us further insight into the role of IL-16 in modulating CNS function. Application of IL-16 alone did not induce an increase in either neuronal or astrocytic $[Ca^{2+}]_i$, which is in contrast to previous studies in T cells where IL-16 induces increases in $[Ca^{2+}]_i$ via IP_3 generation in a CD4-dependent manner (Cruickshank & Center, 1982). Whilst, to the best of our knowledge, this is the first study looking at IL-16 and Ca^{2+} modulation within a CNS preparation, other cytokines including IL-1β and TNF-α have been shown to modulate $[Ca^{2+}]_i$ via a number of mechanisms depending on the cell preparation used (Furukawa and Mattson, 1998; Wuchert et al., 2009; Ghosh et al., 2016). In contrast to the lack of effect on $[Ca^{2+}]_i$ when IL-16 was applied alone, exposure of cultures to IL-16 for 1h resulted in reduced glutamate-induced increases in neuronal $[Ca^{2+}]_i$ but was without effect on glutamate or ADP-induced increases in astrocytic $[Ca^{2+}]_i$. It is well established that glutamate mediates its effects via both ionotropic and metabotropic glutamate receptors. However, as the role of ionotropic glutamate receptors in hippocampal astrocytes remains unclear (Pál, 2018; Rose et al., 2018), our data may indicate that IL-16 selectively modulates neuronally expressed ionotropic glutamate receptors.

4.2. IL-16 reduces the frequency and amplitude of spontaneous EPSCs.

As IL-16 selectively impairs glutamate-induced increases in neuronal $[Ca^{2+}]_i$, we next examined whether IL-16 altered synaptic activity, which is accepted to be glutamate receptor-mediated within hippocampal cultures. Exposure of mouse hippocampal cultures to IL-16, under the same conditions that impaired glutamate-induced Ca^{2+} levels, resulted in a significant decrease in both sEPSC frequency and amplitude. This is the first direct evidence that IL-16 modulates synaptic activity, with both sEPSC frequency and amplitude being reduced, indicating a postsynaptic mechanism of action. This was further confirmed with the finding that GluA1 S831 phosphorylation was reduced with no effect observed on S845 phosphorylation or total GluA1. With GluA1 phosphorylation required for expression in the postsynaptic membrane (Henley and Wilkinson, 2016), our data indicates that reduced postsynaptic GluA1 expression may be a potential mechanism by which IL-16 modulates sEPSCs. Whilst this is the first time that IL-16 has been shown to modulate GluA1, other glutamate receptor subtypes are known to interact with IL-16. Indeed NIL-16 co-immunoprecipitates with the NR2A NMDA subunit when both are overexpressed in cell lines, a finding proposed to be due to NIL-16's PDZ domains (Kurschner and Yuzaki, 1999). The modulation of glutamate receptor function and expression is not unique to IL-16, with other cytokines including IL-1β and TNF-α modulating glutamate receptor function and expression (O'Connor and Coogan, 1999; Viviani et al., 2003; Yang et al., 2005; Liu et al., 2013; Wigerblad et al., 2017). However, in contrast to the reduced GluA1 surface expression induced by IL-16, both IL-1β and TNF-α increase AMPA and NMDA receptor expression and function. Thus, modulation of glutamate receptors may be a common mechanism of action utilised by many cytokines but may be cytokine and region dependent. However, when cultured cerebellar granule neurons (CGN) were exposed to IL-16, this induced expression of the immediate early gene, *c-fos*, (Kurschner and Yuzaki, 1999; Fenster et al., 2010). Given that *c-fos* expression is an indirect marker of increased neuronal activity (Gallo et al., 2018), these data could suggest that IL-16 increases CGN activity. However, no direct electrophysiological measurements were made to examine this, although increased CGN neurite growth was observed, but how this relates to the current findings remains unclear. It should also be noted that the current study focussed solely on sEPSCs, whereas the effects of IL-16 on inhibitory transmission remains unknown. Therefore, any future studies should

4.3. IL-16 impairs Na$^+$ channel function.

Whilst sEPSCs are mediated by spontaneous glutamate release acting on postsynaptic receptors, synaptically-driven action potential firing also contributes to the spontaneous neurotransmitter release observed in hippocampal cultures (Gan et al., 2011; Chanaday and Kavalali, 2018). Therefore, we examined whether IL-16 modulates Na$^+$ and K$^+$ channel function. We reveal for the first time that exposure to IL-16 for 1 hour impairs Na$^+$ channel function but is without effect on K$^+$ channel function. The inhibition of Na$^+$ channel function is not due to reduced Na$^+$ channel expression. Whilst, to the best of our knowledge, this is the first time that a reduction in Na$^+$ channel function has been observed for IL-16, Na$^+$ channel function is modulated in both peripheral and central neurons by other cytokines including IL-1β (Liu et al., 2006; Zhou et al., 2011) and TNF-α (Chen et al., 2015; Leo et al., 2015). In contrast to our knowledge regarding Na$^+$ channel function, NIL-16 interacts with multiple K$^+$ channel subtypes including members of the Kir2 and Kir4 family via its PDZ domain (Kurschner and Yuzaki, 1999). Furthermore, Kv4.2 expression is reduced in the presence of NIL-16 in both COS-7 and hippocampal neurons (Fenster et al., 2007). However, in the present study, IL-16 exposure has no effect on the steady state outward potassium current observed in hippocampal neurons. These data suggest that exposure to IL-16 (1h) can impair neuronal excitability via inhibition of Na$^+$ channel function but is without effect on K$^+$ channel function. In future studies, it would be interesting to examine whether this inhibition is a direct effect on Na$^+$ channels or an indirect effect that develops over time but this is beyond the scope of the present study.

4.4. IL-16-mediated actions in mouse hippocampal neurons are CD4- and CD9-independent.

Under our experimental conditions, CD4 and CD9 were absent in mouse hippocampal cultures, indicating that the observed effects were CD4- and CD9-independent. IL-16 is proposed to modulate neuronal function through both CD4-dependent and -independent pathways (Kurschner and Yuzaki, 1999; Fenster et al., 2010). In a more recent study, CGNs were shown to express CD4 using western

blot and this was absent in CD4-deficient mice (Fenster et al., 2010). Increases in *c-fos* expression following IL-16 treatment were reduced in CD4-deficient mice, whereas increased neurite outgrowth was still present, highlighting that IL-16 mediates its effects through both CD4-dependent and - independent pathways. Furthermore, it has been proposed that IL-16's interaction with immune cells can also be CD4-independent (Mathy et al., 2000), hence our finding that IL-16 mediates its effects in mouse hippocampal cultures via CD4-independent mechanisms is in agreement with this and further supports the idea that other receptors may exist for IL-16 function. Indeed, recent reports have proposed that CD9 may be an alternative receptor via which IL-16 mediates its actions when investigated in lung epithelial and cancer cells (Yadav et al., 2010; Blake et al., 2018). However, our data reveals that similar to CD4, CD9 is not present within our hippocampal cultures and therefore does not underlie the IL-16-mediated effects observed in the present study. We also examined the reported selective IL-16 expression within the brain. In agreement with previous studies (Kurschner and Yuzaki, 1999), we confirmed that IL-16 expression was present in the cerebellum and hippocampus, but also in other regions of the mouse brain. This expression pattern may be due to an IL-16 antibody that is not selective for NIL-16 but is nevertheless interesting given the proposed role of IL-16 in MS and EAE, with IL-16 proposed as a key regulator of the CD4+ T cell mediated immune response in these conditions (Skundric et al., 2015). Given that the cerebellum, and to a lesser extent the hippocampus, are the brain regions where immune cell infiltration occurs in the EAE model (Hridi et al., unpublished observations), our data support the notion that IL-16 may indeed play a key role as a chemoattractant in this inflammation-related CNS disease.

In summary, we provide evidence that exposure of mouse primary hippocampal cultures to IL-16 impairs neuronal excitability and synaptic activity via CD4- and CD9-independent mechanisms. These data extend our current understanding of how IL-16 modulates CNS function and highlight that IL-16 does not function solely via CD4- and CD9-dependent mechanisms, but indicates that alternative targets may be involved.

References

Abdul Rahman NZ, Greenwood SM, Brett RR, Tossell K, Ungless MA, Plevin R, Bushell TJ. 2016. Mitogen-Activated Protein Kinase Phosphatase-2 Deletion Impairs Synaptic Plasticity and Hippocampal-Dependent Memory. J Neurosci. 36:2348-54.

Anvar NE, Saliminejad K, Ohadi M, Kamali K, Daneshmand P, Khorshid HR. 2015. Association between polymorphisms in Interleukin-16 gene and risk of late-onset Alzheimer's disease. J Neurol Sci. 358:324-7.

Arisi GM 2014. Nervous and immune systems signals and connections: cytokines in hippocampus physiology and pathology. Epilepsy Behav. 38:43-7.

Blake DJ, Martiszus JD, Lone TH, Fenster SD. 2018. Ablation of the CD9 receptor in human lung cancer cells using CRISPR/Cas alters migration to chemoattractants including IL-16. Cytokine S1043-4666(18)30238-2.

Center DM, Cruikshank W. 1982. Modulation of lymphocyte migration by human lymphokines. I. Identification and characterization of chemoattractant activity for lymphocytes from mitogen-stimulated mononuclear cells. J Immunol. 128:2563-8.

Chanaday NL, Kavalali ET. 2018. Presynaptic origins of distinct modes of neurotransmitter release. Curr Opin Neurobiol. 51:119-126.

Chen W, Sheng J, Guo J, Gao F, Zhao X, Dai J, Wang G, Li K. 2015. Tumor necrosis factor-α enhances voltage-gated Na$^+$ currents in primary culture of mouse cortical neurons. J Neuroinflammation. 12:126.

Cruickshank, W., Center, D.M., 1982. Modulation of lymphocyte migration by human lymphokines. II. Purification of a lymphocyte factor (LCF). J. Immunol. 128: 2569-74.

Colonna M, Butovsky O. 2017. Microglia function in the central nervous system during health and neurodegeneration. Annu Rev Immunol. 35:441-468.

de Miranda AS, Zhang CJ, Katsumoto A, Teixeira AL. 2017. Hippocampal adult neurogenesis: Does the immune system matter? J Neurol Sci. 372:482-95.

Donzis EJ, Tronson NC. Modulation of learning and memory by cytokines: signaling mechanisms and long term consequences. Neurobiol Learn Mem. 115:68-77.

Elssner A, Doseff AI, Duncan M, Kotur M, Wewers MD. 2004. IL-16 is constitutively present in peripheral blood monocytes and spontaneously released during apoptosis. J Immunol. 172:7721-5.

Fenster CP, Fenster SD, Leahy HP, Kurschner C, Blundon JA. 2007. Modulation of Kv4.2 K+ currents by neuronal interleukin-16, a PDZ domain-containing protein expressed in the hippocampus and cerebellum. Brain Res. 1162:19-31.

Fenster CP, Chisnell HK, Fry CR, Fenster SD. 2010. The role of CD4-dependent signaling in interleukin-16 induced c-Fos expression and facilitation of neurite outgrowth in cerebellar granule neurons. Neurosci Lett. 485:212-6.

Forrester JV, McMenamin PG, Dando SJ. 2018. CNS infection and immune privilege. Nat Rev Neurosci. 19:655-671.

Furukawa K, Mattson MP. 1998. The transcription factor NF-kappaB mediates increases in calcium currents and decreases in NMDA- and AMPA/kainate-induced currents induced by tumor necrosis factor-alpha in hippocampal neurons. J Neurochem. 70:1876-86.

Gallo FT, Katche C, Morici JF, Medina JH, Weisstaub NV. 2018. Immediate early genes, memory and psychiatric disorders: focus on c-Fos, Egr1 and Arc. Front Behav Neurosci. 12:79.

Garcia-Esparcia P, Llorens F, Carmona M, Ferrer I. 2014. Complex deregulation and expression of cytokines and mediators of the immune response in Parkinson's disease brain is region dependent. Brain Pathol. 24:584-98.

Ghosh B, Green MV, Krogh KA, Thayer SA. 2016. Interleukin-1β activates an Src family kinase to stimulate the plasma membrane Ca2+ pump in hippocampal neurons. J Neurophysiol. 115:1875-85.

Gruol DL. 2015. IL-6 regulation of synaptic function in the CNS. Neuropharmacology. 96:42-54.

Henley JM, Wilkinson KA. 2016. Synaptic AMPA receptor composition in development, plasticity and disease. Nat Rev Neurosci. 17:337-50.

Kaser A, Dunzendorfer S, Offner FA, Ludwiczek O, Enrich B, Koch RO, Cruikshank WW, Wiedermann CJ, Tilg H. 2000. B lymphocyte-derived IL-16 attracts dendritic cells and Th cells. J Immunol. 165:2474-80.

Kurschner C, Yuzaki M. 1999. Neuronal interleukin-16 (NIL-16): a dual function PDZ domain protein. J Neurosci. 19:7770-80.

Laurent C, Buée L, Blum D. 2018. Tau and neuroinflammation: What impact for Alzheimer's Disease and Tauopathies? Biomed J. 41:21-33.

Leo M, Argalski S, Schäfers M, Hagenacker T. 2015. Modulation of voltage-gated sodium channels by activation of Tumor Necrosis Factor receptor-1 and receptor-2 in small DRG neurons of rats. Mediators Inflamm. 2015:124942.

Levin SG, Godukhin OV. 2017. Modulating Effect of Cytokines on Mechanisms of Synaptic Plasticity in the Brain. Biochemistry (Mosc). 82:264-274.

Liu Y, Cruikshank WW, O'Loughlin T, O'Reilly P, Center DM, Kornfeld H. 1999. Identification of a CD4 domain required for interleukin-16 binding and lymphocyte activation. J Biol Chem. 274:23387-95.

Liu L, Yang TM, Liedtke W, Simon SA. 2006. Chronic IL-1beta signaling potentiates voltage-dependent sodium currents in trigeminal nociceptive neurons. J Neurophysiol. 95:1478-90.

Liu T, Jiang CY, Fujita T, Luo SW, Kumamoto E. 2013. Enhancement by interleukin-1β of AMPA and NMDA receptor-mediated currents in adult rat spinal superficial dorsal horn neurons. Mol Pain. 9:16.

Louveau A, Harris TH, Kipnis J. 2015 Revisiting the Mechanisms of CNS Immune Privilege. Trends Immunol. 36:569-577.

Martins TB, Rose JW, Jaskowski TD, Wilson AR, Husebye D, Seraj HS, Hill HR. 2011. Analysis of proinflammatory and anti-inflammatory cytokine serum concentrations in patients with multiple sclerosis by using a multiplexed immunoassay. Am J Clin Pathol. 136:696-704.

Mathy NL, Bannert N, Norley SG, Kurth R. 2000. Cutting edge: CD4 is not required for the functional activity of IL-16. J Immunol. 164:4429-32.

O'Connor JJ, Coogan AN. 1999. Actions of the pro-inflammatory cytokine IL-1 beta on central synaptic transmission. Exp Physiol. 84:601-14.

Pál B. 2018. Involvement of extrasynaptic glutamate in physiological and pathophysiological changes of neuronal excitability. Cell Mol Life Sci. doi: 10.1007/s00018-018-2837-5.

Parada NA, Center DM, Kornfeld H, Rodriguez WL, Cook J, Vallen M, Cruikshank WW. 1998. Synergistic activation of CD4+ T cells by IL-16 and IL-2. J Immunol. 160:2115-20.

Ritchie L, Tate R, Chamberlain LH, Robertson G, Zagnoni M, Sposito T, Wray S, Wright JA, Bryant CE, Gay NJ, Bushell TJ. 2018. Toll-like receptor 3 activation impairs excitability and synaptic activity via TRIF signalling in immature rat and human neurons. Neuropharmacology. 135:1-10.

Rose CR, Felix L, Zeug A, Dietrich D, Reiner A, Henneberger C. 2018. Astroglial glutamate signaling and uptake in the hippocampus. Front Mol Neurosci. 10:451.

Selles MC, Oliveira MM, Ferreira ST. 2018. Brain inflammation connects cognitive and non-cognitive symptoms in Alzheimer's disease. J Alzheimers Dis. doi: 10.3233/JAD-179925.

Shrestha R, Millington O, Brewer J, Dev KK, Bushell TJ. 2014. Lymphocyte-mediated neuroprotection in in vitro models of excitotoxicity involves astrocytic activation and the inhibition of MAP kinase signalling pathways. Neuropharmacology. 76:184-93.

Skundric DS, Cruikshank WW, Montgomery PC, Lisak RP, Tse HY. 2015. Emerging role of IL-16 in cytokine-mediated regulation of multiple sclerosis. Cytokine. 75:234-48.

Stephenson J, Nutma E, van der Valk P, Amor S. 2018. Inflammation in CNS neurodegenerative diseases. Immunology. 154:204-219.

Tinning PW, Franssen AJPM, Hridi SU, Bushell TJ, McConnell G. 2018. A 340/380 nm light-emitting diode illuminator for Fura-2 AM ratiometric Ca^{2+} imaging of live cells with better than 5 nM precision. J Microsc. 269:212-220.

Vezzani A, Viviani B. 2015. Neuromodulatory properties of inflammatory cytokines and their impact on neuronal excitability. Neuropharmacology. 96:70-82.

Viviani B, Bartesaghi S, Gardoni F, Vezzani A, Behrens MM, Bartfai T, Binaglia M, Corsini E, Di Luca M, Galli CL, Marinovich M. 2003. Interleukin-1beta enhances NMDA receptor-mediated intracellular calcium increase through activation of the Src family of kinases. J Neurosci. 23:8692-700.

Wigerblad G, Huie JR, Yin HZ, Leinders M, Pritchard RA, Koehrn FJ, Xiao WH, Bennett GJ, Huganir RL, Ferguson AR, Weiss JH, Svensson CI, Sorkin LS. 2017. Inflammation-induced GluA1 trafficking

and membrane insertion of Ca^{2+} permeable AMPA receptors in dorsal horn neurons is dependent on spinal tumor necrosis factor, PI3 kinase and protein kinase A. Exp Neurol. 293:144-58.

Wuchert F, Ott D, Rafalzik S, Roth J, Gerstberger R. 2009. Tumor necrosis factor-alpha, interleukin-1beta and nitric oxide induce calcium transients in distinct populations of cells cultured from the rat area postrema. J Neuroimmunol. 206:44-51.

Yadav S, Shi Y, Wang H. 2010. IL-16 effects on A549 lung epithelial cells: dependence on CD9 as an IL-16 receptor? J Immunotoxicol. 7:183-93.

Yang S, Liu ZW, Wen L, Qiao HF, Zhou WX, Zhang YX. 2005. Interleukin-1beta enhances NMDA receptor-mediated current but inhibits excitatory synaptic transmission. Brain Res. 1034:172-9.

Zéphir H. 2018. Progress in understanding the pathophysiology of multiple sclerosis. Rev Neurol (Paris). pii: S0035-3787(17)30859-7. doi: 10.1016/j.neurol.2018.03.006.

Zheng C, Zhou XW, Wang JZ. 2016. The dual roles of cytokines in Alzheimer's disease: update on interleukins, TNF-α, TGF-β and IFN-γ. Transl Neurodegener. 5:7

Zhou C, Qi C, Zhao J, Wang F, Zhang W, Li C, Jing J, Kang X, Chai Z. 2011. Interleukin-1β inhibits voltage-gated sodium currents in a time- and dose-dependent manner in cortical neurons. Neurochem Res. 36:1116-23.

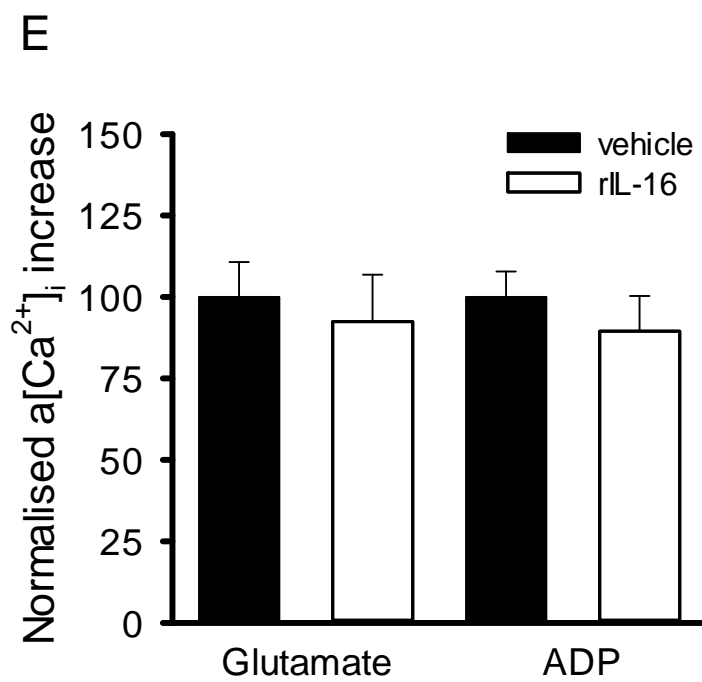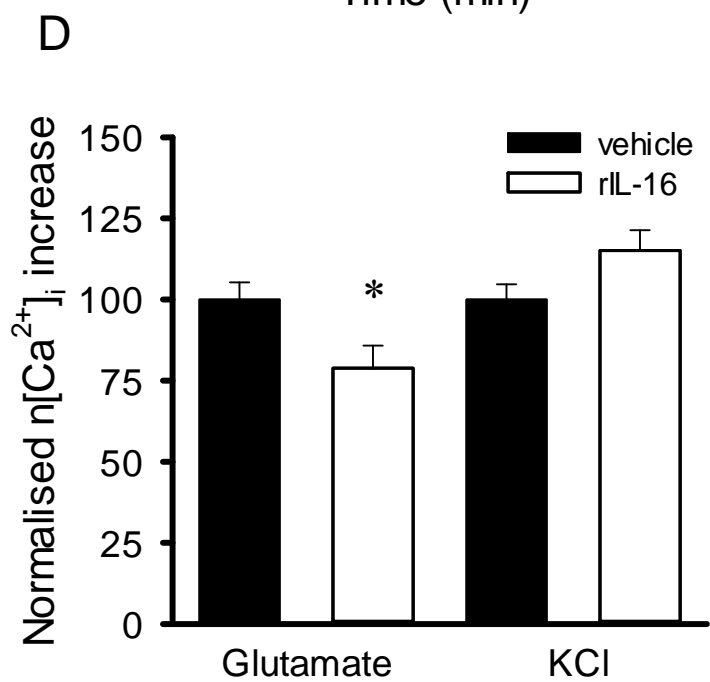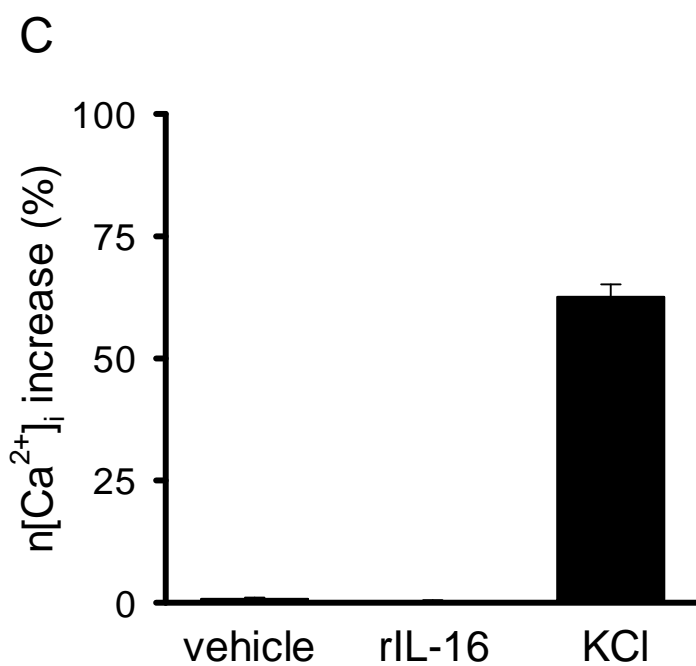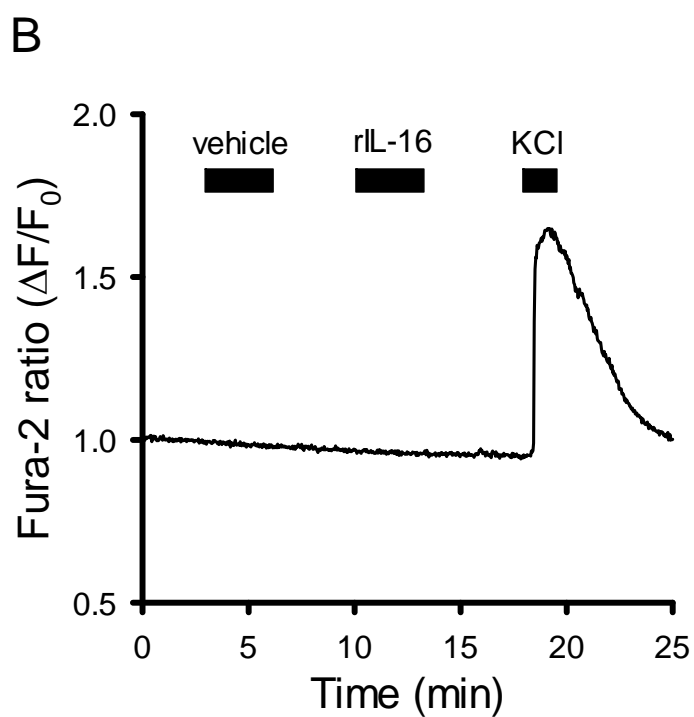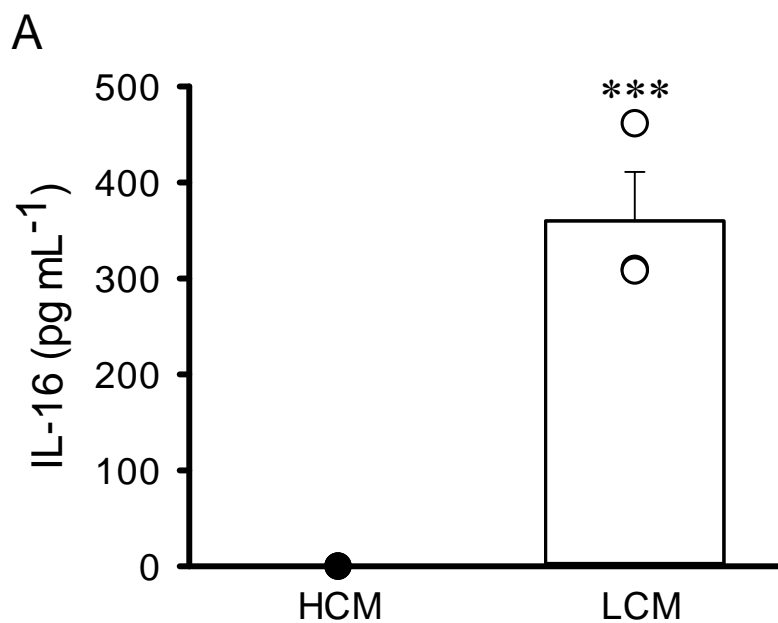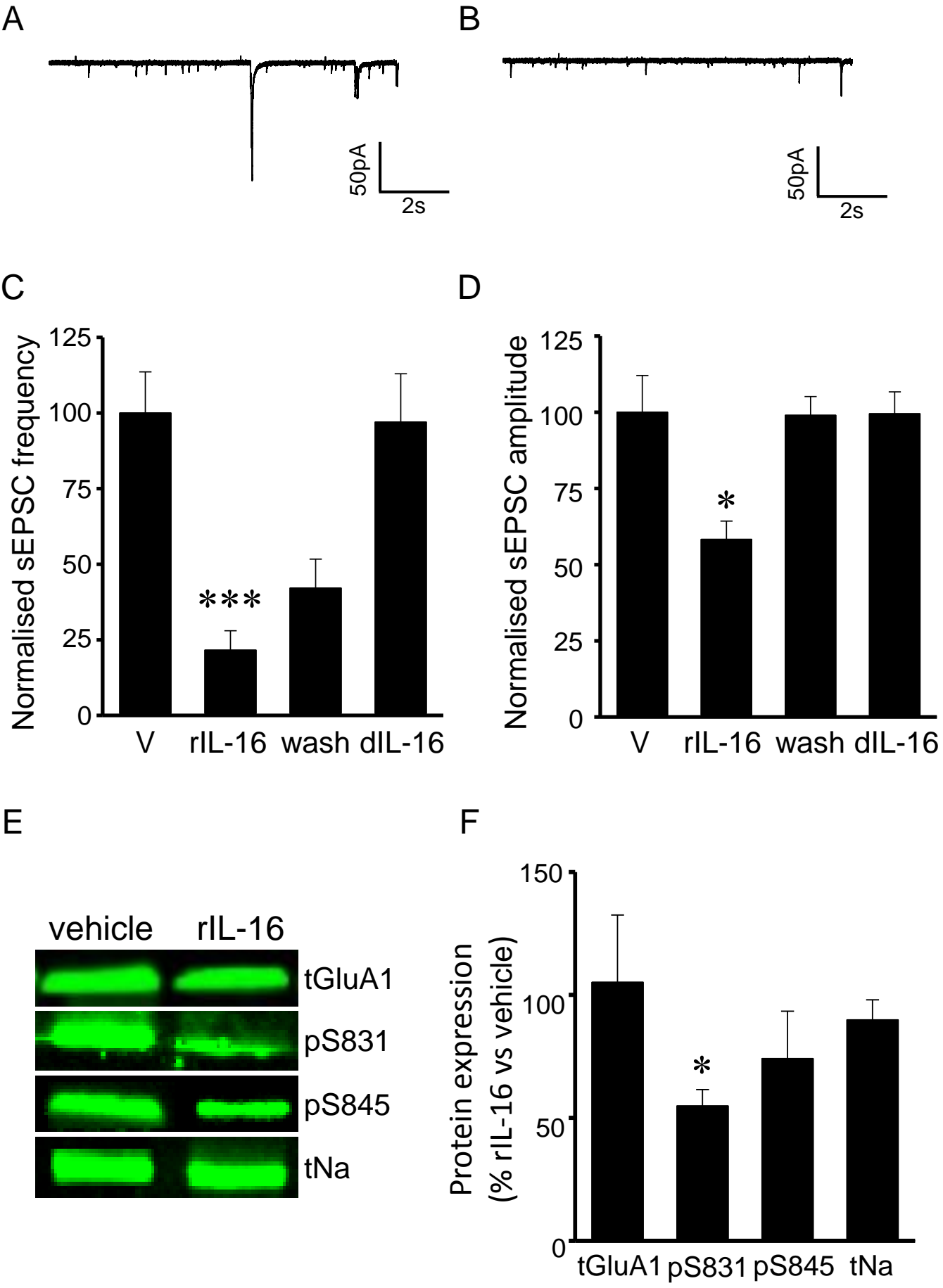**Figure Legends**

Fig. 1. rIL-16 reduces glutamate-induced increases in $n[Ca^{2+}]_i$ levels following a 1-hour treatment. (A) Bar chart revealing that lymphocyte-conditioned media (LCM) contains IL-16. (B + C) Representative trace and bar chart highlighting that rIL-16 (300 pg mL^{-1}, 5 min) does not affect neuronal $[Ca^{2+}]_i$ levels. (D + E) Bar chart revealing that glutamate-induced increases in neuronal $[Ca^{2+}]_i$ levels are reduced by rIL-16 (300 pg mL^{-1}, 1h), whereas no effect was observed in astrocytic $[Ca^{2+}]_i$ levels. *$P < 0.05$ vs vehicle control, ***$P < 0.001$ vs hippocampal conditioned media (HCM) control. Data are mean $\pm$ S.E.M, with n=3 for ELISA and n$\geq$100 cells for Ca^{2+} imaging with each data set taken from at least 3 different cultures.

Fig.2. rIL-16 reduces frequency and amplitude of sEPSCs via impaired GluA1 S831 phosphorylation. (A + B) Representative traces displaying sEPSCs in the absence and presence of rIL-16 (300 pg mL^{-1}, 1h). (C + D) Bar charts revealing effect of rIL-16 (300 pg mL^{-1}, 1h) on sEPSC frequency and amplitude respectively. (E + F) Representative images and bar chart revealing the effects of rIL-16 (300 pg mL^{-1}, 1h) on GluA1 S831 phosphorylation. *$P < 0.05$ vs vehicle control, ***$P < 0.001$ vs vehicle control. Data are mean $\pm$ S.E.M, with n$\geq$6 for sEPSC data and n=3 for western blot data taken from at least 3 different cultures.
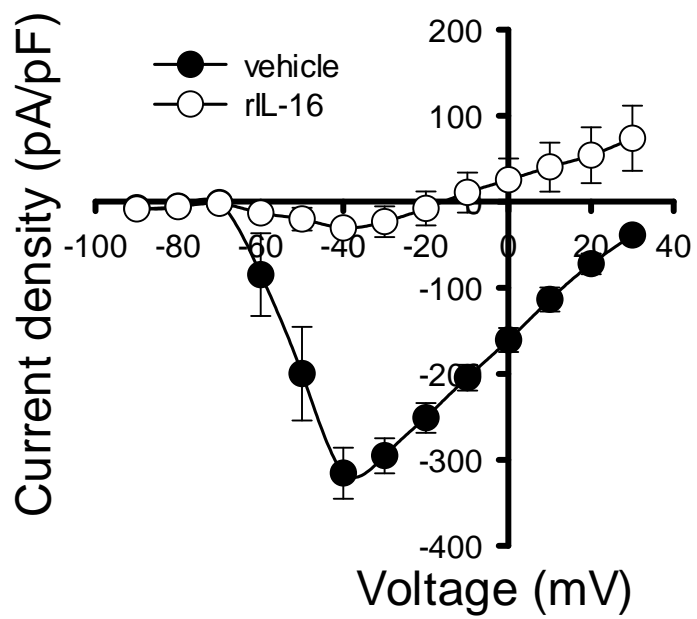
Fig. 3. rIL-16 inhibits Na^+ channel but not K^+ channel function in mouse hippocampal cultures. (A) I-V curve revealing rIL-16 (300 pg mL^{-1}, 1h) inhibits Na^+ current density. (B) I-V curve revealing no effect of rIL-16 (300 pg mL^{-1}, 1h) on K^+ current density. (C) Bar chart summarising the effect of rIL-16 on peak Na^+ current density. (D) Bar chart summarising no effect of rIL-16 on peak K^+ current density. ***$P < 0.001$ vs vehicle control, #$P < 0.05$ vs rIL-16. Data are mean $\pm$ S.E.M, with n$\geq$9 for each data set taken from at least 3 different cultures.

Fig. 4. CD4 receptors are not required for the actions of rIL-16. (A - D) Representative images showing that CD4 staining is absent in both neurons (MAP2 positive) and astrocytes (GFAP positive) present in mouse primary hippocampal cultures. (E - G) Control images revealing that CD4 is present in CD45 expressing lymphocytes. (H + I) Representative images revealing IL-16 expression within the hippocampus and other regions of the mouse brain. (J + K) Representative images highlighting a lack of CD4 expression within the hippocampus and other regions of the mouse brain Scale bars: A - D = 10 μm , E - G = 20 μm , H + J = 500 μm, I + K = 50 μm .
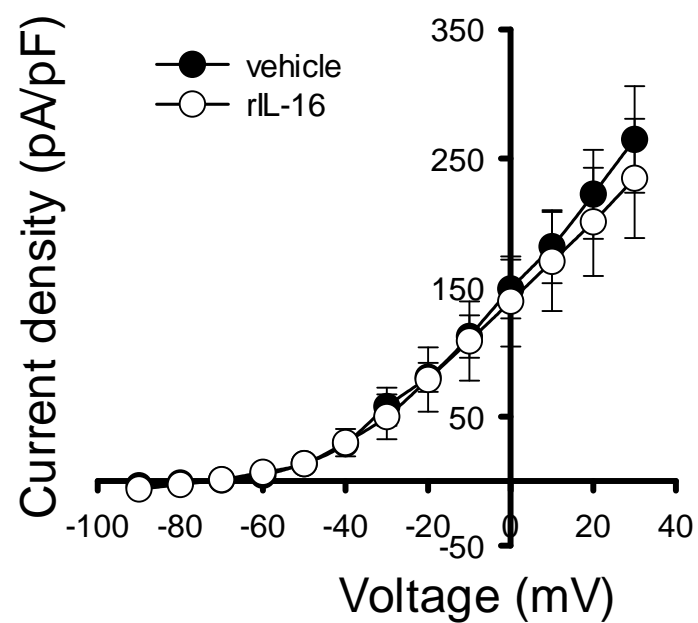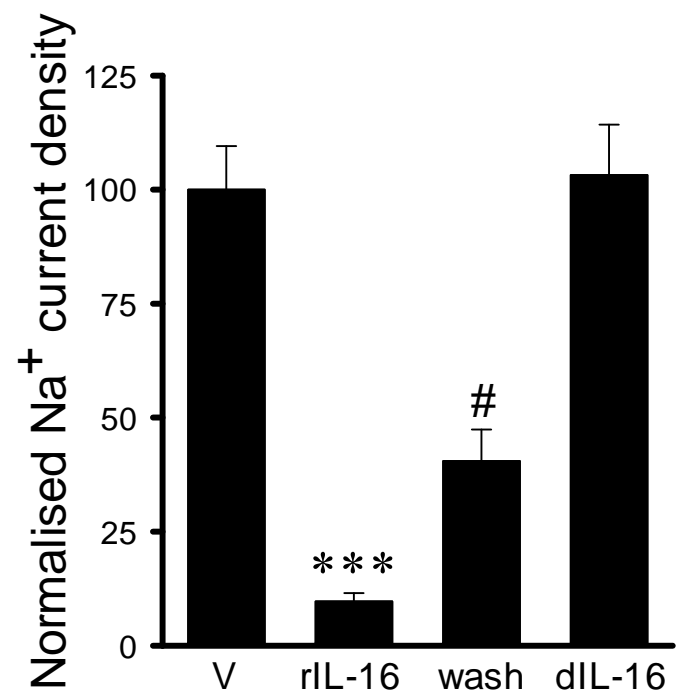
Figure 1

Figure 2

Figure 3

Figure 4